Metabolic Engineering 61 (2020) 381–388

Contents lists available at ScienceDirect

Metabolic Engineering

journal homepage: www.elsevier.com/locate/meteng

Engineering of the 2,3-butanediol pathway of *Paenibacillus polymyxa* DSM 365

Christoph Schilling [a], Rosario Ciccone [a], Volker Sieber [a,b,c,d], Jochen Schmid [a,e,*]

[a] Chair of Chemistry of Biogenic Resources, Technical University of Munich, Campus for Biotechnology and Sustainability, Schulgasse 16, 94315, Straubing, Germany
[b] Fraunhofer IGB, Straubing Branch BioCat, Schulgasse 23, 94315, Straubing, Germany
[c] TUM Catalysis Research Center, Ernst-Otto-Fischer-Straße1, 85748, Garching, Germany
[d] The University of Queensland, School of Chemistry and Molecular Biosciences, 68 Copper Road, St. Lucia, 4072, Australia
[e] Department of Biotechnology and Food Science, Norwegian University of Science and Technology, 7034, Trondheim, Norway

ARTICLE INFO

Keywords:
Butanediol
Paenibacillus polymyxa
Lactate dehydrogenase
Mixed acid pathway
CRISPR-Cas9

ABSTRACT

Paenibacillus polymyxa is a Gram-positive, non-pathogenic soil bacterium that has been extensively investigated for the production of *R-,R*-2,3-butanediol in exceptionally high enantiomeric purity. Rational metabolic engineering efforts to increase productivity and product titers were restricted due to limited genetic accessibility of the organism up to now. By use of CRISPR-Cas9 mediated genome editing, six metabolic mutant variants were generated and compared in batch fermentations for the first time. Downstream processing was facilitated by completely eliminating exopolysaccharide formation through the combined knockout of the *sacB* gene and the *clu1* region, encoding for the underlying enzymatic machinery of levan and paenan synthesis. Spore formation was inhibited by deletion of *spoIIE*, thereby disrupting the sporulation cascade of *P. polymyxa*. Optimization of the carbon flux towards 2,3-butanediol was achieved by deletion of the lactate dehydrogenase *ldh1* and decoupling of the butanediol dehydrogenase from its natural regulation via constitutive episomal expression. The improved strain showed 45 % increased productivity, reaching a final concentration of 43.8 g L^{-1} butanediol. A yield of 0.43 g g^{-1} glucose was achieved, accounting for 86 % of the theoretical maximum.

1. Introduction

2,3-Butanediol (2,3-BDL) is a high value platform chemical with a wide range of applications. In an industrial context, it is most commonly used as a precursor molecule for the conversion to other end products. It can be dehydrated to methyl ethyl ketone, which can be used as a fuel additive or solvent for paints and lacquers. Dehydrogenation yields diacetyl that is industrially utilized in high-value applications as buttery food aroma (Isagulyants and Belomestnykh, 1997). Furthermore, it can be converted to 1,3-butadiene which is applied as a bulk chemical for the production of polymers (Duan et al., 2016). A wide range of applications of 2,3-BDL is also based on its appearance in three stereoisomers – levo-BDL (*R,R*-BDL), dextro-BDL (*S,S*-BDL) and meso-BD (*R,S*-BDL). Particularly the optically active forms, levo-BDL and dextro-BDL are of high industrial interest and can be used for the synthesis of chiral specialty chemicals (Celińska and Grajek, 2009).

Seeking a bio-based industry independent of fossil based resources, there has been a long history of research in biotechnological production of 2,3-BDL (Freeman and Morrison, 1947; Fulmer et al., 1933). A variety of different organisms including *Klebsiella pneumoniae*, *Serratia marcescens, Bacillus* spp. or *Paenibacillus polymyxa* have been shown to produce 2,3-BDL in remarkable amounts. The highest product titer of 152 g L^{-1} with a productivity of 4.2 g L^{-1} h^{-1} has been described by *K. pneumoniae* in fed-batch fermentations (Ma et al., 2009). Remarkable titers of 139 g L^{-1} were also obtained with *S. marcescens* (Zhang et al., 2010). However, the pathogenic nature of *K. pneumoniae* and *S. marcescens,* which defines them a risk class 2 organism limits their utilization for industrial scale production processes. In contrast, *Bacillus* spp. such as *B. amyloliquefaciens* and *B. licheniformis* are generally regarded as safe (GRAS) and have also demonstrated high 2,3-BDL titers (Jurchescu et al., 2013; Yang et al., 2011). However, mainly the optical inactive meso-BDL isomer is produced by these organisms. Interestingly, high titers of 2,3-BDL up to 98 % purity can be produced by the Gram-positive, non-pathogenic, spore forming, soil bacterium *P. polymyxa* under microaerobic conditions and therefore represents a promising starting point for future optimization (Huo et al., 2010; Jeong

Abbreviations: 2,3-BDL, 2,3-butanediol; CDW, cell dry weight; wt, wildtype.

* Corresponding author. Chair of Chemistry of Biogenic Resources, Technical University of Munich, Campus for Biotechnology and Sustainability, Schulgasse 16, 94315, Straubing, Germany.

https://doi.org/10.1016/j.ymben.2020.07.009
Received 3 June 2020; Received in revised form 12 July 2020; Accepted 27 July 2020
Available online 7 August 2020

et al., 2019; Nakashimada et al., 1998).

The biosynthesis of 2,3-BDL follows a mixed acid fermentative pathway at microaerobic conditions (Fig. 1) (Ji et al., 2011a). In short, one mol of glucose is converted to pyruvate by the simultaneous generation of two mols of ATP and NADH via glycolysis. Consequently, two mol of pyruvate are converted to α-acetolactate, which is further decarboxylated to acetoin and finally dehydrogenated to butanediol while simultaneously one redox equivalent of NAD^+ is produced (Fig. 1). In absence of alternative electron acceptors during anaerobic and microaerobic conditions, the redox balance is maintained by the formation of additional side products (Clark, 1989). Depending on oxygen availability, lactate dehydrogenase, pyruvate formate lyase as well as the pyruvate dehydrogenase complex compete for the intermediate pyruvate. This finally results in the production of lactate, formate, ethanol or acidic acid (Alexeeva et al., 2003; Nakashimada et al., 1998).

The production of butanediol in *P. polymyxa* has been extensively studied towards improved process parameters and media composition (Häßler et al., 2012; Laube et al., 1984a, 1984b; Okonkwo et al., 2017b). While other organisms have been successfully engineered on a molecular level in order to increase the overall 2,3-BDL production, previous efforts on this in *P. polymyxa* were restricted due to its limited genetic accessibility. Based on our recently developed tool for CRISPR-Cas9 mediated genome editing in *P. polymyxa* DSM 365 (Rütering et al., 2017) we performed in this work the first intensified rational metabolic engineering of *Paenibacillus polymyxa* towards an increased 2,3-BDL biosynthesis. The focus of this study was to address aspects of downstream processing such as increased viscosity due to exopolysaccharide production or spore formation. *P. polymyxa* is known for the production of the exopolysaccharide (EPS) levan when growing on sucrose and a heteropolysaccharide named paenan when grown on monomeric carbohydrates such as glucose (Rütering et al., 2016). Both polymers can interfere with the downstream processing due to the increased viscosity of the fermentation broth and also can impair mass transfer during fermentation (Häßler et al., 2012). In addition, *P. polymyxa* forms metabolically dormant endospores as a stress response, which do not contribute to butanediol or EPS formation (Dworkin and Shah, 2010). Furthermore, spores represent a severe issue of bio-based industrial scale processes in which genetically modified organisms are used and any leakage from the manufacturing plant in form of product contamination must be prevented. Thus, sporulation should be eliminated without negatively impacting 2,3-BDL formation. Interestingly, the sporulation cascade in *P. polymyxa* differs from the well described cascade in *B. subtilis*. Particularly histidine kinases, which sense sporulation-specific signals and initiate a phosphorelay reaction are only poorly conserved or completely missing and require further investigation (Park et al., 2012).

Besides downstream impeding by-products such as EPS or spores, the mixed acid pathway itself should be engineered to redirect carbon flux from other side products towards 2,3-BDL in context of a rational metabolic engineering approach. 2,3-BDL constitutes a toxic end product in higher concentrations for the producing organism and biosynthesis is tightly regulated (Okonkwo et al., 2017a). Consequently, deregulation of the pathway might allow to overcome this bottleneck in *P. polymyxa*. Overexpression of genes involved in the butanediol pathway (Guo et al., 2014; Lu et al., 2010; Yang et al., 2013) or deletion of side products directly branching from the pathway, which affect redox equivalents and improve the carbon flux towards 2,3-BDL have previously proven to be valid strategies in other organism (Ji et al., 2011b; Yang et al., 2015; Zhang et al., 2018). In this study, we evaluated the effects of rational metabolic engineering strategies of the mixed-acid pathway on 2,3-BDL biosynthesis by a comparative experimental setup in *P. polymyxa* DSM 365 for the first time.

2. Materials and methods

2.1. Strain

P. polymyxa DSM 365 was acquired from the German Collection of Microorganisms and Cell Culture (DSMZ), Braunschweig, Germany. *Escherichia coli* NEB Turbo cells (New England Biolabs, USA) were used for any plasmid construction presented in this study. *E. coli* S17-1 (DSMZ strain DSM 9079) was used for transformation of *P. polymyxa* DSM 365 via conjugation. All strains were grown in LB media (5 g L^{-1} yeast extract, 10 g L^{-1} tryptone, 10 g L^{-1} NaCl) and additionally supplemented with 50 μg ml^{-1} neomycin and 20 μg ml^{-1} polymyxin if required. All strains were stored in 30 % glycerol at −80 °C. Prior to liquid cultivation, strains were streaked on LB agar plates and incubated at 30 °C. All strains used or constructed in this study are listed in Table S1.

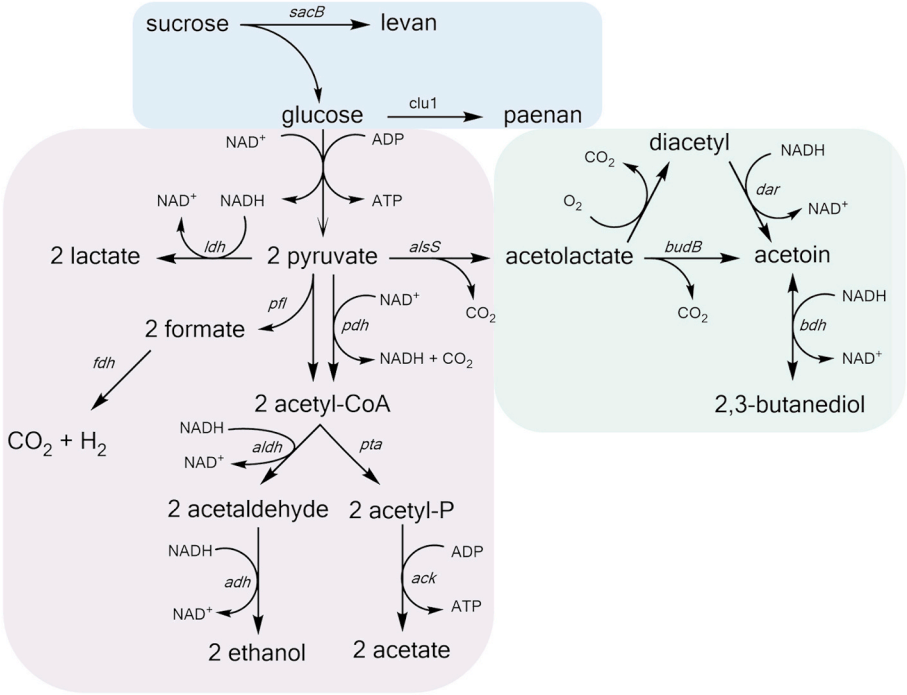

Fig. 1. Overview of 2,3-BDL biosynthesis pathway and byproducts in microaerobic conditions of *P. polymyxa* DSM 365 starting from sucrose as a substrate. Sucrose can be converted to the homopolysaccharide levan or to the heteroexopolysaccharide paenan. Butanediol is produced in a mixed acid fermentation pathway starting from pyruvate. Other side products such as lactate, ethanol, acetate or formate are competing over pyruvate as a substrate. Blue: polysaccharide synthesis, green: butanediol pathway, purple: mixed acid pathway, *sacB*: levansucrase, clu1: operon responsible for the production of paenan, *fdh*: formate dehydrogenase; *alsS*: acetolactate synthase; *budB*: acetolactate decarboxylase; *dar*: diacetyl reductase; *bdh*: butanediol dehydrogenase *aldh*: acetaldehyde dehydrogenase; *adh*: alcohol dehydrogenase; *pta*: phosphate acetyltransferase; *ack*: acetate kinase. (For interpretation of the references to colour in this figure legend, the reader is referred to the Web version of this article).

2.2. CRISPR-Cas9 mediated genome editing

All gene knock-outs were performed as previously described (Rütering et al., 2017). In brief, gRNAs for the targeted genome regions were designed using Benchling CRISPR Design Tool. Oligonucleotides were phosphorylated, annealed and cloned into pCasPP by Golden Gate assembly. Approximately 1 kB up- and downstream homology flanks for each targeted nucleotide sequence were amplified from genomic DNA of *P. polymyxa* DSM 365, fused via overlap extension PCR and cloned into pCasPP after linearization by use of SpeI. After transformation of *E. coli* NEB Turbo, clones were analyzed for correct construct assembly by colony PCR (cPCR) and sequencing of the amplicons. Finally, correct constructs (Table S2) were transferred to chemical competent *E. coli* S17-1 cells for the following conjugational transfer to *P. polymyxa*. All primers used for the construction of the knockout plasmids are listed in Table S3. For each target, two gRNAs were tested and listed in the supplemental material if successful.

2.3. Conjugation based transformation of P. polymyxa DSM 365

P. polymyxa was transformed by conjugation using *E. coli* S17-1 harboring the various plasmids. Overnight cultures of donor and recipient strains were diluted 1:100 with selective or non-selective LB media respectively and cultivated at 37 °C for 3 h, 280 rpm. 900 µl of the recipient culture was heat shocked at 42 °C for 15 min and mixed with 300 µl of the donor strain. Cells were centrifuged at 6000 g for 2 min, resuspended in 400 µl LB media and dropped on non-selective LB agar plates. After 24 h of incubation at 30 °C, cells were scrapped off, resuspended in 500 µl LB-broth and 100 µl thereof were plated on selective LB-agar containing 50 µg ml^{-1} neomycin and 20 µg ml^{-1} polymyxin for counter selection. *P. polymyxa* conjugants were analyzed for successful transformation after 48 h incubation at 30 °C by cPCR. Confirmed knock out strains were plasmid cured by cultivation in LB broth at 37 °C without antibiotic selection pressure and subsequent replica plating on LB agar plates both with and without neomycin. Strains that did not grow on plates with selection marker were verified by sequencing of the target region and used for further experiments.

2.4. Fermentation media

All medium components were obtained from Carl Roth GmbH (Germany) if not indicated differently. Medium composition was adapted from a previous study (Okonkwo et al., 2017b). A single colony was used for inoculation of 50 ml pre-culture medium containing 60 g L^{-1} glucose, 5 g L^{-1} yeast extract, 5 g L^{-1} tryptone, 0.2 g L^{-1} $MgSO_4x7\,H_2O$ (Sigma Aldrich, USA), 3.5 g L^{-1} KH_2PO_4, 2.5 g L^{-1} K_2HPO_4. Fermentation medium components were autoclaved separately and contained 120 g L^{-1} glucose, 7 g L^{-1} glycerol, 5 g L^{-1} yeast extract, 3.5 g L^{-1} tryptone, 0.2 g L^{-1} $MgSO_4x7\,H_2O$, 3.5 g L^{-1} KH_2PO4, 2.5 g L^{-1} K_2HPO_4, 5 g L^{-1} ammonium acetate, 4 g L^{-1} $(NH_4)_2SO_4$ and 3 ml L^{-1} trace elements. Trace element solution contained 2.5 g L^{-1} iron sulfate heptahydrate, 2.1 g L^{-1} sodium tartrate dihydrate, 1.8 g L^{-1} manganese chloride dihydrate, 0.075 g L^{-1} cobalt chloride hexahydrate, 0.031 g L^{-1} copper sulfate pentahydrate, 0.258 g L^{-1} boric acid, 0.023 g L^{-1} sodium molybdate dihydrate and 0.021 g L^{-1} zinc chloride. Trace element solution was filter-sterilized and added to the media after cooling down to room temperature.

2.5. Batch fermentation

Batch fermentations were conducted in 1 L DASGIP bioreactors (Eppendorf, Germany) with an initial volume of 550 ml. A single colony from a freshly streaked plate was used to inoculate 100 ml pre-culture medium by following incubation for 16 h at 30 °C, 160 rpm. 50 ml of this cultivation broth (diluted with pre-culture medium if necessary) were used to inoculate the bioreactor by an initial OD_{600} of 0.1. Fermentation was performed at 35 °C and constant aeration of 0.075 vvm. The stirrer was equipped with a 6-plate-rushton impeller placed 4 cm from the bottom of the shaft and constantly stirring at 300 rpm. The pH value was maintained at 6.0 and automatically adjusted with 2 M NaOH or 1.35 M H_3PO_4 as required. Foam control was performed using 1 % of antifoam B (Merck, Germany). For monitoring the process parameters, reactors were equipped with redox and pH probes. Oxygen transfer rate (OTR) and carbon dioxide production rate (CPR) were determined by online off-gas measurements by a DASGIP GA4 exhaust gas analyzer (Eppendorf, Germany). Under the assumption of pseudo-steady state and oxygen limited conditions, in which liquid gas concentrations are close to zero, the oxygen uptake rate (OUR) can be assumed as followed (Eq. (1)):

$$OUR = OTR - \frac{tc_L}{td} \triangleq OTR \quad (1)$$

Respiratory quotient (RQ) was calculated based on OUR and CPR (Eq. (2)):

$$RQ = \frac{CPR}{OUR} \quad (2)$$

2.6. Continuous fermentation

Continuous fermentations were performed in 2 L reactors (Sartorius Biostat B plus, Sartorius AG, Germany) with a constant volume of 1.5 L. Aeration, agitation and temperature parameters were kept identical to the previously described batch fermentation. The pH value was maintained at 6.0 and automatically adjusted with 2 M NaOH or 1.35 M H_3PO_4 as required. For monitoring the process parameters, reactors were equipped with redox and pH probes. Foam control was performed using 1 % of antifoam B. Two 6-plate-rushton impellers were placed 3 cm and 6 cm from the bottom respectively. Continuous flow started 24 h after inoculation with a constant dilution of 0.042 h^{-1} and fermentation medium containing 46.2 g L^{-1} of glucose. Cell retention was guaranteed by use of a 0.2 µm filtration probe (TRACE analytics, Germany). Steady-state was assumed when product concentrations remained constant for at least 24 h.

2.7. Analytical methods

Cell growth was determined by measuring optical density at 600 nm (OD_{600}) using a Ultraspec 10 spectrophotometer (Amersham Biosciences, UK). For cell dry weight determination, 1 ml of fermentation broth was centrifuged at 24,000 g for 5 min. The resulting supernatant was filtered with 0.2 µm PTFE filters and utilized for HPLC-UV-RID analysis. The remaining cell pellet was dried over night at 105 °C. Living cell count was determined by serial dilutions of the fermentation broth with 0.9 % NaCl and appropriate plating on LB-agar plates. Colony forming units were determined after 48 h of incubation at 30 °C. Glucose and product concentrations were determined via a HPLC-UV-RID system (Dionex, USA) equipped with Rezex ROA-H^+ organic acid column (300 mm × 7.8 mm Phenomenex, USA). Column temperature was set to 70 °C and 2.5 mM H_2SO_4 was used as the mobile phase with a flow rate of 0.5 ml min^{-1}. All measured concentrations of 2,3-BDL in this publication represent solely the levo-stereoisomer of the alcohol if not explicitly noted differently. EPS concentrations were determined by centrifugation (8000 g, 15 min) of 100 ml aliquots of fermentation broth at the end of the cultivation process. Supernatant was slowly poured into 200 ml of isopropanol while stirring. Precipitated EPS was collected, dried overnight in a VDL53 vacuum oven at 40 °C (Binder, Germany) and following gravimetrical weight determination.

2.8. Sporulation assay

Five ml of LB medium were inoculated with 1 % preculture of the respective *P. polymyxa* strain and incubated at 37 °C, 300 rpm for 4 days. 500 µl of the culture broth were transferred to 1.5 ml reaction tubes and

incubated at 85 °C in a water bath. Serial dilutions were afterwards plated on LB-agar plates and incubated at 30 °C for two days in order to determine the colony forming units (cfu).

3. Results and discussion

3.1. Construction of knock out variants

Knockout constructs were generated to eliminate undesirable side-products of 2,3-BDL fermentations. EPS formation was targeted by deletion of a heteroexopolysaccharide cluster (*clu1*) combined with the levansucrase *sacB*. Sporulation was inhibited by deletions of key steps in the sporulation cascade, *spo0A* and *spoIIE*. In order to target metabolic pyruvate drains to redirect the carbon flux towards 2,3-BDL production pyruvate formate lyase (*pfl*) and a lactate dehydrogenase were deleted. Open reading frames of each targeted gene were completely removed by homologous repair assisted mechanisms mediated by CRISPR-Cas9 using 1 kb flanks up- and downstream of the target region, which were provided by the pCasPP plasmid. Deletion of each target was confirmed by cPCR and further verified by sequencing (Fig. S1). After plasmid curing, all verified knockout variants were evaluated and compared via 72 h batch fermentations for their yield in 2,3-BDL production as well as side product formation (Fig. 2). In addition, the process characteristics were analyzed (Table 1). The results of each generated metabolic mutant variant are discussed individually in the sections below.

3.2. Deletion of EPS formation

Recently, it has been shown that deletion of *sacB*, encoding for a levansucrase forming the fructose based carbohydrate polymer levan from sucrose, had a positive impact on 2,3-BDL synthesis (Okonkwo et al., 2020). However, *P. polymyxa* is known to produce an additional heteroexopolysaccharide, which might additionally interfere with the downstream processing of the targeted product 2,3-BDL (Rütering et al., 2016). In order to redirect the carbon flux towards butanediol formation, essential parts of the operon, responsible for the heteropolysaccharide biosynthesis (*clu1*) were deleted in addition to the *sacB* gene. As a result, no EPS formation was observed, and the cell growth was directly affected (Table 1). Both, OD_{600} and CDW increased over the course of the batch fermentation compared to the wildtype strain, but the final 2,3-BDL titer remained nearly unaffected (Fig. S3). However, lactate production was increased by 70 %, while the BDL-yield was slightly decreased to 0.37 g g^{-1} (Fig. S4). In previous studies (Häßler et al., 2012; Okonkwo et al., 2017b) EPS concentrations of 5–54 g L^{-1} were reported using similar cultivation conditions to our experimental set up. Compared to previous studies, the obtained EPS concentrationsin this study were generally very low with approximately 450 mg L^{-1} for the wildtype strain by use of the DASGIP bioreactors. Utilization of glucose as a carbon source already prevented levan production such giving BDL titers of up to 54 g L^{-1} (Häßler et al., 2012). In combination with low aeration and low inoculum volume, this resulted in only small amounts of heteroexopolysaccharide formation by *P. polymyxa*. Nevertheless, by genetic engineering it was possible for the first time to completely eliminate EPS formation in *P. polymyxa* by use of the Δ*clu1 ΔsacB* strain. However, it appeared that only minor amounts of carbon could be successfully redirected towards 2,3-BDL production (Fig. 2). Despite higher biomass and increased OD_{600} values after 72 h of batch cultivation, the final 2,3-BDL titer of 30.39 g L^{-1} remained comparable to the wildtype strain (Table 1). While the glucose consumption slightly increased, mostof the carbon source was redirected to the non-toxic end product lactate, rather than 2,3-BDL (Table S6).

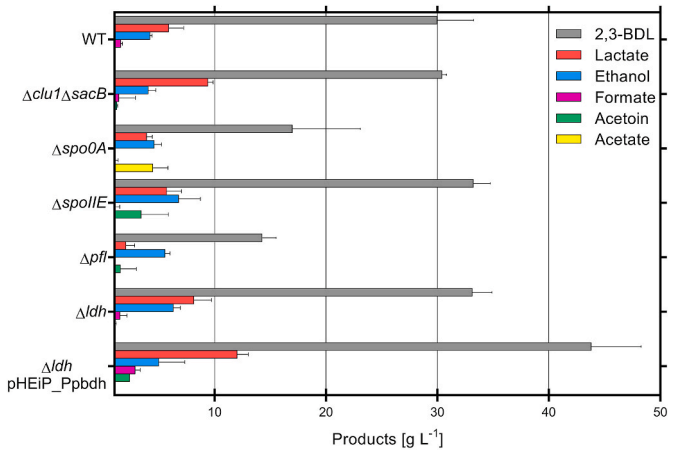

Fig. 2. Product profiles of *P. polymyxa* DSM 365 wt and engineered variants after 72 h of controlled batch cultivation in DASGIP bioreactors applying microaerobic conditions (0.075 vvm). Engineering of EPS formation (*Δclu1 ΔsacB*), sporulation (*ΔspoA*, *ΔspoIIE*), or the mixed acid pathway (*Δpfl*, *Δldh*) altered the final product titer of 2,3-BDL and side products. Plasmid based overexpression of butanediol dehydrogenase increased 2,3-BDL concentration by 46 %. Product concentrations are the result of three independent fermentation processes.

3.3. Deletion of spore formation

To prevent initiation of the sporulation cascade, *spo0A* encoding the corresponding sporulation stage 0 master transcription factor that initiates the sporulation cascade upon phosphorylation (Fujita et al., 2005), was deleted. As a result, no spores were detected within the sporulation assay and microscopic analysis for any sample taken during the batch fermentations (Table S5). However, the growth rate of 0.225 h^{-1} of the *ΔspoA* mutant was significantly reduced compared to 0.311 h^{-1} of the wildtype (Table 1). For *P. polymyxa* wt and all other knockout variants, the stationary phase of the batch fermentations was reached within the first 24 h. The *spo0A* knockout variant continued to show exponential growth at later stages and only surpassed OD and CDW values of the wildtype strain towards the end of the process (Figure S3). In parallel, formation of 2,3-BDL was strongly affected. After 72 h of batch fermentation, only 16.97 g L^{-1} of 2,3-BDL were obtained (Fig. 2). The wildtype of P. polymyxa exclusively produced R,R-BDL under microaerobic conditions, whereas for the *spo0A* knockout variant elevated concentrations of 0.6 g L-*1* meso-BDL where obtained. As a result, enantiomeric purity of R,R-BD decreased to 96.5 %. I *B. subtilis,* Spo0A is known to directly or indirectly influence the expression of over 500 genes, which might explain the negative impact on BDL-biosynthesis (Molle et al., 2003). No consensus binding sites of Spo0A can be found in close proximity to any gene of the butanediol pathway, but Spo0A has been shown to control the expression of several other transcription factors. RAST (Rapid Annotation using Subsystem Technology) analysis (Overbeek et al., 2014) of the genome of *P. polymyxa* revealed only one single butanediol dehydrogenase, which belongs to the medium-chain dehydrogenase/reductase family known to form the R-alcohol (Yu et al., 2011). Meso-BDL is expected to be formed by spontaneous conversion of acetolactate to diacetyl and the following transformation to S-acetoin by diacetylreductase (Haukeli and Lie, 1978; Zhang et al., 2018). Therefore, we hypothesize that the master regulator Spo0A indirectly affects butanediol synthesis in *P. polymyxa* by downregulation of acetolactate decarboxylase. Consequently, less *R, R*-BDL is produced, while in contrast more S-acetoin is formed. Interestingly, butanediol dehydrogenase accepts both acetoin enantiomers as a substrate (Yu et al., 2011) and can thus further convert S-acetoin to meso-BDL resulting in a lower enantiomeric purity.

In addition to 2,3-BDL synthesis, the *spo0A* deletion had an impact on the acetate metabolism (Fig. S4). Initial acetate levels have been shown to shift mixed acid fermentation towards the synthesis of butanediol (Nakashimada et al., 2000; Yu and Saddler, 1985) and were therefore part of the media composition. While all other strains used in this study consumed initial acetate to the end of the growth phase, the *spo0A* deletion mutant did not deplete acetate at all. Instead, the concentration slightly

Table 1
Overview of process characteristics *of P. polymyxa* DSM 365 wt and metabolic mutant variants. Results were obtained by three independent 72 h batch fermentations at microaerobic conditions. The CDW was determined after 72 h of cultivation from a single bioreactor.

Strain	Y_{PS} [g g^{-1}]	Productivity [g L^{-1} h^{-1}]	CDW [g L^{-1}]	μ [h^{-1}]	2,3-BDLTiter [g L^{-1}]	EPS [mg L^{-1}]
wt	0.42 ± 0.01	0.42 ± 0.04	3.40 ± 0.12	0.311 ± 0.026	29.96 ± 2.69	443 ± 48
Δ*clu1* Δ*sacB*	0.37 ± 0.02	0.42 ± 0.00	4.60 ± 0.17	0.330 ± 0.012	30.39 ± 0.34	0 ± 0
Δ*spo0A*	0.23 ± 0.08	0.24 ± 0.07	4.80 ± 0.14	0.225 ± 0.019	16.97 ± 4.99	240 ± 14
Δ*spoIIE*	0.36 ± 0.02	0.46 ± 0.02	4.70 ± 0.26	0.337 ± 0.012	33.21 ± 1.25	413 ± 12
Δ*pfl*	0.25 ± 0.07	0.20 ± 0.01	2.73 ± 0.57	0.125 ± 0.014	14.24 ± 1.04	187 ± 17
Δ*ldh1*	0.39 ± 0.01	0.46 ± 0.02	5.40 ± 0.95	0.295 ± 0.015	33.11 ± 1.44	480 ± 22
Δ*ldh1* pHEiP_Ppbdh	0.43 ± 0.06	0.61 ± 0.05	4.93 ± 0.41	0.290 ± 0.026	43.80 ± 3.66	403 ± 12

increased. Studies conducted in *Clostridium cellulolyticum* and *C. beijerinckii* revealed that the shift from acetogenesis to solvent formation in these organism was controlled by Spo0A. (Ravagnani et al., 2000). While the precise mechanism of Spo0A influencing mixed acid fermentation in *P. polymyxa* has not been extensively investigated yet, we assume that the transcription factor putatively acts in a similar way as in *Clostridium* spp. Consequently, the knockout of *spo0A* partially redirected the carbon flux from butanediol towards acetate.

Due to the observed negative global effects of *spo0A* deletion on 2,3-BDL synthesis, a second gene downstream of the sporulation cascade, not known to interfere with other metabolic pathways was targeted. The *spoIIE* gene encodes a serine phosphatase involved in the early stage II sporulation phase (Bi et al., 2011; Scotcher and Bennett, 2005). As a result of the knockout, no spore formation could be observed in the batch fermentation and negative effects on the mixed-acid metabolism of *P. polymyxa* were eliminated. The yield slightly decreased to 0.36 g g^{-1}, however the final titer of 33.21 g L^{-1} was similar to the wildtype strain (Table 1). While deletion of *spo0A* had a negative impact on biomass formation, the *spoIIE* mutant did not show decreased cell growth (Fig. S3). Instead, a rather slightly increased biomass formation was observed, which might explain the 10 % increased 2,3-BDL concentration at the end of batch fermentation.

Deficiency in spore formation was proven by heat treatment of cultures grown for 4 days in LB broth (Table S4). While the wildtype strain survived 45 min of heat exposure at 85 °C, both sporulation knockout variants Δ*spo0A* and Δ*spoIIE* did not display any vegetative cell growth after the same time of heat treatment. Thus, spore free mutants were successfully established by gene deletion-based disruption of the sporulation cascade. Due to multiple negative side effects of the deletion of the master regulator Spo0A, only *P. polymyxa* Δ*spoIIE* proved to be suitable for butanediol production.

3.4. Elimination of formate formation

At anaerobic and microaerobic conditions, glucose is converted to pyruvate through the Embden-Meyerhof-Parnas pathway, which then branches and the three enzymes, lactate dehydrogenase, pyruvate formate lyase as well as acetoacetate synthase compete for the intermediate pyruvate. The expression level of the individual enzymes highly depends on the oxygen availability under microaerobic conditions (De Mas et al., 1988; Nakashimada et al., 1998). Deletion of *pfl* has previously been shown to be an efficient strategy to increase 2,3-BDL production by decreasing formate formation (Jung et al., 2014). Only minor levels of formate were detected for all investigated strains of this study. However, formate can be further converted to CO_2 and H_2 by formate dehydrogenase, thus removing the intermediate from the fermentation broth. Deletion of *pfl* indeed resulted in the complete elimination of formate (Fig. 2). Although, cell growth was severely reduced and OD_{600} as well as cell dry weight were decreased by 46 % and 19 % respectively compared to the wild type (Table 1). Consequently, the 2,3-BDL titer was also significantly attenuated to 14.21 g L^{-1}. Decreased 2,3-BDL concentrations were not only a result of lower biomass, but also the product yield was reduced significantly compared to other mutant variants as well as the wild type. At microaerobic conditions, both pyruvate formate lyase (Pfl) and the pyruvate dehydrogenase complex (Pdhc) compete for the intermediate pyruvate (Alexeeva et al., 2003). In comparison to previous studies for 2,3-BDL optimization, the applied aeration of 0.075 vvm was rather low explaining the shift towards *pfl* expression. Pyruvate formate lyase represents a redox valve, that can compensate for the redox imbalance of the butanediol pathway (Adlakha et al., 2015). Consequently, the decreased cell growth might be a result of intracellular redox imbalance as well as the limited availability of acetyl-CoA, which is also a key intermediate in the biosynthesis of fatty acids (Krivoruchko et al., 2015). Due to the low 2,3-BDL yield and volumetric productivity of the Δ*pfl* strain, no further characterization of this strain was conducted even though we demonstrated that the formate production can be completely omitted.

3.5. Knockout of a lactate dehydrogenase to redirect the carbon flux

The most prominent side product under the applied condition was lactate. In sum, four putative genes encoding lactate dehydrogenases were identified by RAST analysis of the genome of *P. polymyxa* DSM 365. Out of those genes, *ldh1* showed 60.19 % sequence identity to *ldh1* of *B. subtilis* and was therefore chosen as a target in order to remove or reduce lactate formation as a by-product (Hecker et al., 2009). However, during batch fermentations no attenuation of the lactate concentrations could be observed (Fig. S4). The final butanediol titer after 72 h of fermentation slightly increased by 10 % towards 33.11 g L^{-1}, but also lactate concentration was significantly elevated (Fig. 2). Based on our results, we concluded that the remaining three putative lactate dehydrogenases in *P. polymyxa* DSM 365 might compensate the deletion of *ldh1*. Interestingly, OD_{600} as well as the cell dry weight was significantly

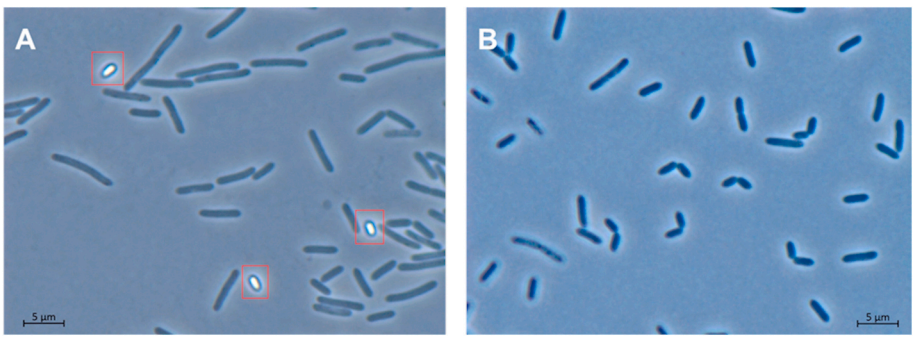

Fig. 3. Phase-contrast microscopic image (100× magnifications, Axio Observer Z1, Zeiss, Germany) of a 24 h *P. polymyxa* wt (A) and Δ*ldh1* (B) culture in pre-culture medium at 30 °C and 300 rpm. The wildtype strain showed matured rod-shaped cell morphology, while Δ*ldh1* formed averaged smaller cells that were observed in a permanent stage of cell division. Spores are marked by red rectangles. (For interpretation of the references to colour in this figure legend, the reader is referred to the Web version of this article).

Table 2
Substrate consumption and product formation rates of *P. polymyxa* DSM 365 wt and Δ*ldh1* in continuous process mode with a dilution rate of 0.042 h^{-1} during steady-state conditions.

Volumetric rates [g L^{-1} h^{-1}]							
Strain	r_{Gluc}	r_{BDL}	$r_{Ethanol}$	$r_{Acetate}$	$r_{Acetoin}$	$r_{Lactate}$	OD_{600}
wt	−1.87 ± 0.03	0.60 ± 0.03	0.19 ± 0.01	−0.13 ± 0.02	0.05 ± 0.01	0.02 ± 0.00	6.9 ± 0.10
Δldh1	−1.99 ± 0.08	0.90 ± 0.03	0.31 ± 0.01	−0.13 ± 0.01	0.03 ± 0.00	0.17 ± 0.02	14.9 ± 0.10

increased compared to the wildtype strain (Table 1). Additionally, the early stage productivity of fermentation prior to product inhibition was significantly increased. Microscopic analysis of the fermentation broth (Fig. 3) revealed that the wildtype strain mainly formed matured cells with an average length of 5.4 μm (n = 19). In contrast, the Δ*ldh1* mutant showed most cells in a permanent stage of cell division, thus reducing the average length to 3.3 μm (n = 17). Additionally, no spore formation was observed over the whole course of the fermentation. Contrary, the wildtype strain did show spore formation, even in early stages of the fermentation course. The exact mechanism for this behavior remains to be investigated but similar effects have previously been described for *Enterobacter aerogenes, K. pneumoniae and B. subtilis* (Guo et al., 2014; Jung et al., 2012; Lu et al., 2010; Yang et al., 2015).

For further investigation of the effects of *ldh1* knockout on the productivity of *P. polymyxa* DSM 365, the knockout as well as the wildtype strain were cultivated in a continuous reactor system with cell retention to reduce effects of product inhibition on the organism. When product concentration remained constant for a minimum of 24 h, cells were considered in steady-state and production rates were calculated (Table 2).

Although the glucose consumption rate slightly increased from 1.87 g L^{-1} for the wildtype to 1.99 g L^{-1} for the Δ*ldh*1 variant, the butanediol production rate increased by 50 % from 0.60 to 0.90 g L^{-1} h^{-1}. Maximal OD_{600} values of Δ*ldh*1 were significantly higher with maximum values of 15 compared to 7 for the wildtype strain. Further, the cell dry mass increased by 25 % to 5.31 g L^{-1} in comparison to 4.24 g L^{-1} for the wildtype. Thus, the increase in optical density values could be mostly attributed to the different light scattering caused by changed cell morphology. Living cell count was increased 4.4-fold, thus confirming the presence of many more small cells rather than a few larger cells (Fig. 4).

3.6. Decoupling of butanediol dehydrogenase increased productivity

During the continuous process mode, a constant production rate of 0.90 g L^{-1} h^{-1} under low product concentrations was observed for the Δ*ldh1* strain. (Table 2). In batch fermentations, productivity in the early phase of fermentation reached similar values (Fig. S3). However, after an initial peak in production until 24 h, the production rates declined (Fig. S3). This is particularly based on the downregulation of the expression of the butanediol dehydrogenase (*bdh*) which is in correlation with increasing acetoin concentrations. In order to evaluate this observation, a plasmid encoding a PSP01-*bdh* expression cassette for the constitutive expression of bdh was designed and transferred to *P. polymyxa Δldh1* (Lee et al., 1980) (Fig. S2). Overexpression of *bdh* has previously been shown to positively impact 2,3-BDL production in *B. amyloliquefaciens* (Yang et al., 2013). Batch fermentation of, *P. polymyxa* Δ*ldh1* pHEiP_Ppbdh showed that the formation of side products such as ethanol or lactate were not affected and similar titers as for the Δ*ldh1* variant without additional expression of *bdh* were obtained (Fig. 2). Solely acetoin concentrations at the end of the cultivation were significantly increased from 0.96 g L^{-1} to 2.35 g L^{-1}. Furthermore, OD_{600} as well as CDW remained comparable to the parent strain indicating a neglectable metabolic burden by the constitutively plasmid-based expression (Table 1).

In the early process phase, no significant differences in the production rates of 2,3-BDL were observed. Volumetric productivity remained high until a product concentration of about 30 g L^{-1} was reached, resulting in a final space time yield (STY) of 0.61 g L^{-1} h-^{1} at 72 h after inoculation (Fig. 4 A). In contrast, the volumetric productivity of the wildtype strain without episomal expression of *Ppbdh* already declined after an initial spike surpassing 10 g L^{-1} of the product. Over the complete process a significantly reduced productivity of 0.42 g L^{-1} h^{-1} was obtained. Therefore, it is concluded that *bdh* expression was successfully decoupled from the native regulation system resulting in a 45 % increased volumetric productivity in *P. polymyxa Δldh1* pHEiP_Ppbdh. The respiratory quotient (RQ) is a parameter to easily monitor productivity in anaerobic and microaerobic process conditions (Zeng et al., 1994). After an initial increase of the RQ peak at 17 h after inoculation, values of the wildtype strain quickly dropped to a level of 2 and remained constant for the rest of the process. The initial spike has previously been associated with increased ethanol production proceeding butanediol biosynthesis in *B. licheniformis*,

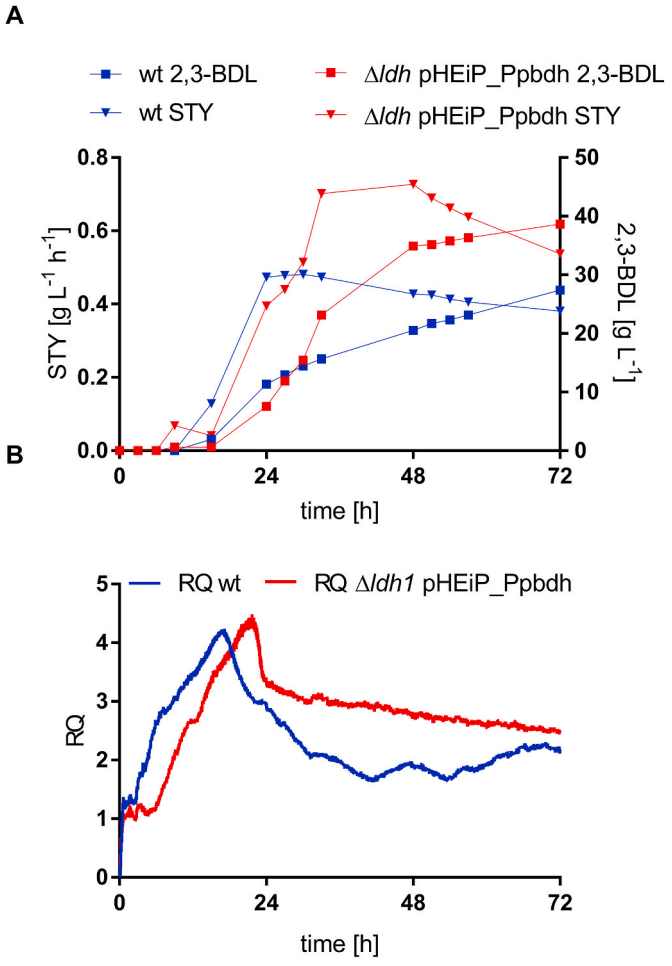

Fig. 4. A) Space time yield (STY) of 2,3-BDL over the course of a 72 h batch cultivation (n = 1). The wildtype productivity (blue) stagnated at 0.45 g L^{-1} h^{-1} after reaching a product titer of 10 g L^{-1}, while *ldh1* pHEiP_Ppbdh (red) with decoupled *bdh* expression showed significantly increased productivity, which only declined after surpassing 30 g L^{-1} 2,3-BDL. Triangles: STY; Squares: 2,3-BDL titer B) Increased productivity was reflected in the respiratory quotient (RQ). Decoupled expression of *bdh* led to increased RQ values over the course of the fermentation, while in the wildtype strain CO_2 production rates quickly dropped after reaching inhibitory 2,3-BDL concentrations. (For interpretation of the references to colour in this figure legend, the reader is referred to the Web version of this article).

which could be also observed in *P. polymyxa* (Heyman et al., 2020). In contrast to the wildtype, the strain with decoupled *bdh* expression reached higher product concentrations, which was also reflected in higher RQ values only slowly declining subsequent to the initial peak emergence (Fig. 5 B). For that reason, the monitoring of the RQ moreover confirmed higher metabolic activity of *P. polymyxa Δldh1* pHEiP_Ppbdh.

Shaking flask experiments in *B. licheniformis* showed the active conversion of 2,3-BDL to acetoin after the complete consumption of glucose by the reversed reaction of butanediol dehydrogenase (Heyman et al., 2020).*P. polymyxa* Δ*ldh1* pHEiP_Ppbdh also accumulated increased concentrations of 2.35 g L^{-1} acetoin compared to 0.86 g L^{-1} in the wildtype strain after 72 h of fermentation. However, in the same time frame glucose was never fully depleted in any fermentation process and also no decrease in 2,3-BDL was determined for *P. polymyxa* Δ*ldh1* pHEiP_Ppbdh. Even though the volumetric productivity was increased in our experiments, a 2,3-BDL mediated feedback inhibition was still observed at higher product concentrations indicating additional regulatory mechanisms limiting the production of butanediol.

Due to the redox imbalance of butanediol synthesis, other pathways are required to ensure NAD^+ equilibrium. When the NAD^+/NADH balance cannot be restored otherwise under microaerobic conditions, glucose is converted to redox-neutral end products such as ethanol and lactate. Pyruvate formate lyase enables conversion of pyruvate to acetyl-CoA without generating any redox equivalents. Subsequently, two mols of NAD^+ are regenerated by the combined action of aldehyde dehydrogenase and alcohol dehydrogenase. This route represents the most efficient pathway for redox regeneration in *P. polymyxa* which allows for the compensation of the redox imbalance of the butanediol biosynthesis (Adlakha et al., 2015). Interestingly, in *P. polymyxa* Δ*ldh1* pHEiP_Ppbdh the redox balance was not accomplished by expanding the carbon flux towards ethanol. (Table S6). However, pyruvate was used for the redox neutral production of lactate. With declining productivity of 2,3-BDL after approximately 48 h of cultivation, lactate formation started to result in a final titer of 12.0 g L^{-1} (Fig. 5, Table S4). Ethanol production is more efficient for the redox balance, but also represents additional solvent stress next to 2,3-BDL. Even though the conversion of pyruvate to lactate yields only one mol NAD^+ per mol substrate, solvent stress mitigation by production of lactate seemed to be favorable in pH-controlled bioreactor cultivations. In contrast, the more efficient ethanol formation was favored over lactate production during continuous fermentation mode of *P. polymyxa* Δ*ldh1*, in which both products ethanol and 2,3-BDL were constantly removed from the fermentation broth. Therefore, we conclude that not only oxygen supply but also alcohol concentration is highly important for the regulation of the mixed acid pathway in *P. polymyxa*.

Previous studies have demonstrated a toxicity threshold concentration of 50 g L^{-1} 2,3-BDL for *P. polymyxa* (Okonkwo et al., 2017a). Due to the toxicity of 2,3-BDL, an economically feasible process might not be easily achieved without further engineering strategies in *P. polymyxa*. Notably, other studies demonstrated significantly higher 2,3-BDL titers of up to 150 g L^{-1} for *Bacillus* strains such as *B. amyloliquefaciens* and *B. licheniformis* (Jurchescu et al., 2013; Yang et al., 2011). A better understanding of the underlying resistance mechanism of these strains is required to further engineer *P. polymyxa* towards similar product titers.

Even so, by overexpression of *bdh* in *P. polymyxa Δldh1* we successfully demonstrated the possibility of decoupling the last enzymatic step in butanediol formation. Most importantly we were able to increase the productivity of 2,3-BDL by 45 % compared to the wildtype strain.

4. Conclusion

P. polymyxa revealed to be an highly interesting GRAS platform organism with the advantage of producing exceptionally pure *R,R*–BDL. Based on our recently developed novel CRISPR-Cas9 mediated genome editing tools this study represents the first targeted approach of rational metabolic engineering of *P. polymyxa* DSM 365 for a simplified downstream processing of 2,3-BDL by complete elimination of EPS production

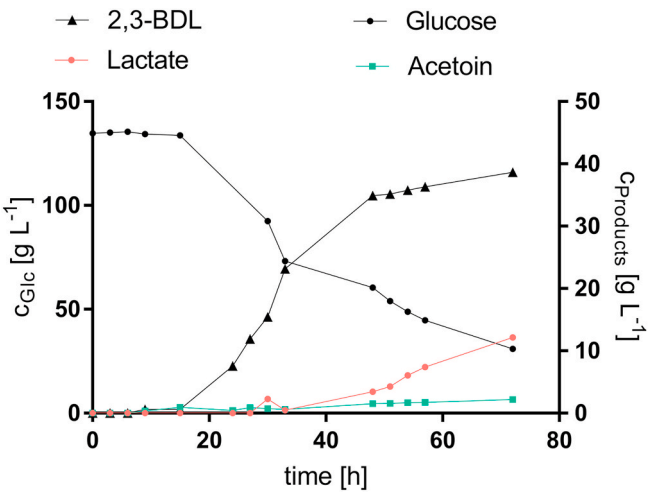

Fig. 5. Production of 2,3-BDL (black triangles) in *P. polymyxa* DSM 365 Δ*ldh* pHEiP_Ppbdh showed increased productivity. After 48 h acetoin (green) started to accumulate while also lactate biosynthesis (red) was induced to ensure a redox neutral end product for glucose. (For interpretation of the references to colour in this figure legend, the reader is referred to the Web version of this article).

as well as spore formation. Six mutant variants were generated to comparatively study the effects on the 2,3-BDL metabolism in *P. polymyxa* DSM 365. For the first time, EPS formation was eliminated by the combined knockout of the cluster responsible for heteroexopolysaccharide synthesis and the levansucrase SacB. Furthermore, we demonstrated that deletion of the sporulation stage 0 transcription factor Spo0A negatively impacted 2,3-BDL formation as well as the enantiomeric purity of the diol. However, sporulation was successfully inhibited by the knockout of *spoIIE* without affecting 2,3-BDL synthesis. In addition, by deletion of *ldh1*, which showed the highest similarity to the lactate dehydrogenase, proved to be responsible for lactate production in *B. subtilis*, we realized a completely different growth behavior of *P. polymyxa* in combination with reduction of spore formation. By that, we were able to obtain much higher cell densities, product titers as well as cell viability. This represents a highly promising approach towards optimized production strains, by massive engineering of the native growth behavior, what might be transferred to already established production strains, to further increase the efficiency.

While similar strategies to engineer the mixed acid pathway have been applied in *Klebsiella sp.* and *Enterobacter sp.*, we demonstrated that not all of them could be universally transferred to *P. polymyxa*. Novel insight of the metabolism of this organism at microaerobic conditions and the role of key enzymes such as Pfl were obtained, further contributing to future research on this interesting alternative host organism and closely related *Bacillus* species. Finally, rational modification of the mixed acid pathway and flux optimization towards butanediol by decoupling the expression of *bdh* resulted in a strain with 45 % increased productivity and 2,3-BDL titer.

Author statement

Christoph Schilling, Jochen Schmid: Conceptualization, Methodology, **Rosario Ciccone, Christoph Schilling, Jochen Schmid:** Experiments, Data Analysis, Writing- Original draft preparation. **Jochen Schmid:** Supervision.: **Rosario Ciccone, Christoph Schilling, Jochen Schmid, Volker Sieber:** Writing- Reviewing and Editing.

Appendix A. Supplementary data

Supplementary data to this article can be found online at https://doi.org/10.1016/j.ymben.2020.07.009.

References

Adlakha, N., Pfau, T., Ebenhöh, O., Yazdani, S.S., 2015. Insight into metabolic pathways of the potential biofuel producer, *Paenibacillus polymyxa* ICGEB2008. Biotechnol. Biofuels 8, 159. https://doi.org/10.1186/s13068-015-0338-4.

Alexeeva, S., Hellingwerf, K.J., Teixeira de Mattos, M.J., 2003. Requirement of ArcA for redox regulation in *Escherichia coli* under microaerobic but not anaerobic or aerobic conditions. J. Bacteriol. 185, 204–209. https://doi.org/10.1128/JB.185.1.204-209.2003.

Bi, C., Jones, S.W., Hess, D.R., Tracy, B.P., Papoutsakis, E.T., 2011. SpoIIE is necessary for asymmetric division, sporulation, and expression of F, E, and G but does not control solvent production in *Clostridium acetobutylicum* ATCC 824. J. Bacteriol. 193, 5130–5137. https://doi.org/10.1128/JB.05474-11.

Celińska, E., Grajek, W., 2009. Biotechnological production of 2,3-butanediol—current state and prospects. Biotechnol. Adv. 27, 715–725. https://doi.org/10.1016/j.biotechadv.2009.05.002.

Clark, D.P., 1989. The fermentation pathways of *Escherichia coli*. FEMS Microbiol. Lett. 63, 223–234. https://doi.org/10.1111/j.1574-6968.1989.tb03398.x.

De Mas, C., Jansen, N.B., Tsao, G.T., 1988. Production of optically active 2,3-butanediol by *Bacillus polymyxa*. Biotechnol. Bioeng. 31, 366–377. https://doi.org/10.1002/bit.260310413.

Duan, H., Yamada, Y., Sato, S., 2016. Future prospect of the production of 1,3-butadiene from butanediols. Chem. Lett. 45, 1036–1047. https://doi.org/10.1246/cl.160595.

Dworkin, J., Shah, I.M., 2010. Exit from dormancy in microbial organisms. Nat. Rev. Microbiol. 8, 890–896. https://doi.org/10.1038/nrmicro2453.

Freeman, G.G., Morrison, K.I., 1947. Production of 2:3-butylene glycol by fermentation of molasses. J. Soc. Chem. Ind. 66, 216–221. https://doi.org/10.1002/jctb.5000660706.

Fujita, M., Gonzalez-Pastor, J.E., Losick, R., 2005. High- and low-threshold genes in the Spo0A regulon of *Bacillus subtilis*. J. Bacteriol. 187, 1357–1368. https://doi.org/10.1128/JB.187.4.1357-1368.2005.

Fulmer, E.I., Christensen, L.M., Kendali, A.R., 1933. Production of 2,3-butylene glycol by fermentation. Ind. Eng. Chem. 25, 798–800. https://doi.org/10.1021/ie50283a019.

Guo, X.-W., Zhang, Y.-H., Cao, C.-H., Shen, T., Wu, M.-Y., Chen, Y.-F., Zhang, C.-Y., Xiao, D.-G., 2014. Enhanced production of 2,3-butanediol by overexpressing acetolactate synthase and acetoin reductase in *Klebsiella pneumoniae*: enhanced Production of 2,3-Butanediol. Biotechnol. Appl. Biochem. 61, 707–715. https://doi.org/10.1002/bab.1217.

Häßler, T., Schieder, D., Pfaller, R., Faulstich, M., Sieber, V., 2012. Enhanced fed-batch fermentation of 2,3-butanediol by *Paenibacillus polymyxa* DSM 365. Bioresour. Technol. 124, 237–244. https://doi.org/10.1016/j.biortech.2012.08.047.

Haukeli, A.D., Lie, S., 1978. Conversion of α-acetolactate and removal of diacetyl A kinetic study. J. Inst. Brew. 84, 85–89. https://doi.org/10.1002/j.2050-0416.1978.tb03843.x.

Hecker, M., Reder, A., Fuchs, S., Pagels, M., Engelmann, S., 2009. Physiological proteomics and stress/starvation responses in *Bacillus subtilis* and *Staphylococcus aureus*. Res. Microbiol. 160, 245–258. https://doi.org/10.1016/j.resmic.2009.03.008.

Heyman, B., Tulke, H., Putri, S.P., Fukusaki, E., Büchs, J., 2020. Online monitoring of the respiratory quotient reveals metabolic phases during microaerobic 2,3-butanediol production with *Bacillus licheniformis*. Eng. Life Sci. 20, 133–144. https://doi.org/10.1002/elsc.201900121.

Huo, Z., Yang, X., Raza, W., Huang, Q., Xu, Y., Shen, Q., 2010. Investigation of factors influencing spore germination of *Paenibacillus polymyxa* ACCC10252 and SQR-21. Appl. Microbiol. Biotechnol. 87, 527–536. https://doi.org/10.1007/s00253-010-2520-8.

Isagulyants, G.V., Belomestnykh, I.P., 1997. Butadione synthesis by dehydrogenation and oxidative dehydrogenation of 2,3-butanediol. In: Studies in Surface Science and Catalysis. Elsevier, pp. 415–420. https://doi.org/10.1016/S0167-2991(97)80932-9.

Jeong, H., Choi, S.-K., Ryu, C.-M., Park, S.-H., 2019. Chronicle of a soil bacterium: *Paenibacillus polymyx*a E681 as a tiny guardian of plant and human health. Front. Microbiol. 10, 467. https://doi.org/10.3389/fmicb.2019.00467.

Ji, X.-J., Huang, H., Ouyang, P.-K., 2011a. Microbial 2,3-butanediol production: a state-of-the-art review. Biotechnol. Adv. 29, 351–364. https://doi.org/10.1016/j.biotechadv.2011.01.007.

Ji, X.-J., Nie, Z.-K., Huang, H., Ren, L.-J., Peng, C., Ouyang, P.-K., 2011b. Elimination of carbon catabolite repression in *Klebsiella oxytoca* for efficient 2,3-butanediol production from glucose–xylose mixtures. Appl. Microbiol. Biotechnol. 89, 1119–1125. https://doi.org/10.1007/s00253-010-2940-5.

Jung, M.-Y., Mazumdar, S., Shin, S.H., Yang, K.-S., Lee, J., Oh, M.-K., 2014. Improvement of 2,3-butanediol yield in *Klebsiella pneumoniae* by deletion of the pyruvate formate-lyase gene. Appl. Environ. Microbiol. 80, 6195–6203. https://doi.org/10.1128/AEM.02069-14.

Jung, M.-Y., Ng, C.Y., Song, H., Lee, J., Oh, M.-K., 2012. Deletion of lactate dehydrogenase in *Enterobacter aerogenes* to enhance 2,3-butanediol production. Appl. Microbiol. Biotechnol. 95, 461–469. https://doi.org/10.1007/s00253-012-3883-9.

Jurchescu, I.-M., Hamann, J., Zhou, X., Ortmann, T., Kuenz, A., Prüße, U., Lang, S., 2013. Enhanced 2,3-butanediol production in fed-batch cultures of free and immobilized *Bacillus licheniformis* DSM 8785. Appl. Microbiol. Biotechnol. 97, 6715–6723. https://doi.org/10.1007/s00253-013-4981-z.

Krivoruchko, A., Zhang, Y., Siewers, V., Chen, Y., Nielsen, J., 2015. Microbial acetyl-CoA metabolism and metabolic engineering. Metab. Eng. 28, 28–42. https://doi.org/10.1016/j.ymben.2014.11.009.

Laube, V.M., Groleau, D., Martin, S.M., 1984a. The effect of yeast extract on the fermentation of glucose to 2,3-butanediol by *Bacillus polymyxa*. Biotechnol. Lett. 6, 535–540. https://doi.org/10.1007/BF00139998.

Laube, V.M., Groleau, D., Martin, S.M., 1984b. 2,3-Butanediol production from xylose and other hemicellulosic components by *Bacillus polymyxa*. Biotechnol. Lett. 6, 257–262. https://doi.org/10.1007/BF00140047.

Lu, Y., Zhao, H., Zhang, C., Lai, Q., Wu, X., Xing, X.-H., 2010. Alteration of hydrogen metabolism of ldh-deleted *Enterobacter aerogenes* by overexpression of NAD(+)-dependent formate dehydrogenase. Appl. Microbiol. Biotechnol. 86, 255–262. https://doi.org/10.1007/s00253-009-2274-3.

Ma, C., Wang, A., Qin, J., Li, L., Ai, X., Jiang, T., Tang, H., Xu, P., 2009. Enhanced 2,3-butanediol production by *Klebsiella pneumoniae* SDM. Appl. Microbiol. Biotechnol. 82, 49–57. https://doi.org/10.1007/s00253-008-1732-7.

Molle, V., Fujita, M., Jensen, S.T., Eichenberger, P., González-Pastor, J.E., Liu, J.S., Losick, R., 2003. The Spo0A regulon of *Bacillus subtilis*: the Spo0A regulon. Mol. Microbiol. 50, 1683–1701. https://doi.org/10.1046/j.1365-2958.2003.03818.x.

Nakashimada, Y., Kanai, K., Nishio, N., 1998. Optimization of dilution rate, pH and oxygen supply on optical purity of 2, 3-butanediol produced by *Paenibacillus polymyxa* in chemostat culture. Biotechnol. Lett. 20, 1133–1138. https://doi.org/10.1023/A:1005324403186.

Nakashimada, Y., Marwoto, B., Kashiwamura, T., Kakizono, T., Nishio, N., 2000. Enhanced 2,3-butanediol production by addition of acetic acid in *Paenibacillus polymyxa*. J. Biosci. Bioeng. 90, 661–664. https://doi.org/10.1016/S1389-1723(00)90013-6.

Okonkwo, C., Ujor, V., Cornish, K., Ezeji, T.C., 2020. Inactivation of levansucrase gene in *Paenibacillus polymyxa* DSM 365 diminishes exopolysaccharide biosynthesis during 2,3-butanediol fermentation. Appl. Environ. Microbiol. AEM. https://doi.org/10.1128/AEM.00196-20, 00196-20, aem;AEM.00196-20v1.

Okonkwo, C., Ujor, V., Ezeji, T.C., 2017a. Investigation of relationship between 2,3-butanediol toxicity and production during growth of *Paenibacillus polymyxa*. N. Biotech. 34, 23–31. https://doi.org/10.1016/j.nbt.2016.10.006.

Okonkwo, C., Ujor, V., Mishra, P., Ezeji, T., 2017b. Process development for enhanced 2,3-butanediol production by *Paenibacillus polymyxa* DSM 365. Fermentation 3, 18. https://doi.org/10.3390/fermentation3020018.

Overbeek, R., Olson, R., Pusch, G.D., Olsen, G.J., Davis, J.J., Disz, T., Edwards, R.A., Gerdes, S., Parrello, B., Shukla, M., Vonstein, V., Wattam, A.R., Xia, F., Stevens, R., 2014. The SEED and the rapid annotation of microbial genomes using subsystems Technology (RAST). Nucleic Acids Res. 42, D206–D214. https://doi.org/10.1093/nar/gkt1226.

Park, S.-Y., Park, S.-H., Choi, S.-K., 2012. Characterization of sporulation histidine kinases of *Paenibacillus polymyxa*. Res. Microbiol. 163, 272–278. https://doi.org/10.1016/j.resmic.2012.02.003.

Ravagnani, A., Jennert, K.C.B., Steiner, E., Grunberg, R., Jefferies, J.R., Wilkinson, S.R., Young, D.I., Tidswell, E.C., Brown, D.P., Youngman, P., Morris, J.G., Young, M., 2000. Spo0A directly controls the switch from acid to solvent production in solvent-forming clostridia. Mol. Microbiol. 37, 1172–1185. https://doi.org/10.1046/j.1365-2958.2000.02071.x.

Rütering, M., Cress, B.F., Schilling, M., Rühmann, B., Koffas, M.A.G., Sieber, V., Schmid, J., 2017. Tailor-made exopolysaccharides—CRISPR-Cas9 mediated genome editing in *Paenibacillus polymyxa*. Synth. Biol. 2 https://doi.org/10.1093/synbio/ysx007.

Rütering, M., Schmid, J., Rühmann, B., Schilling, M., Sieber, V., 2016. Controlled production of polysaccharides–exploiting nutrient supply for levan and heteropolysaccharide formation in *Paenibacillus* sp. Carbohydr. Polym. 148, 326–334. https://doi.org/10.1016/j.carbpol.2016.04.074.

Scotcher, M.C., Bennett, G.N., 2005. SpoIIE regulates sporulation but does not directly affect solventogenesis in *Clostridium acetobutylicum* ATCC 824. J. Bacteriol. 187, 1930–1936. https://doi.org/10.1128/JB.187.6.1930-1936.2005.

Yang, T., Rao, Z., Hu, G., Zhang, X., Liu, M., Dai, Y., Xu, M., Xu, Z., Yang, S.-T., 2015. Metabolic engineering of *Bacillus subtilis* for redistributing the carbon flux to 2,3-butanediol by manipulating NADH levels. Biotechnol. Biofuels 8. https://doi.org/10.1186/s13068-015-0320-1.

Yang, T., Rao, Z., Zhang, X., Lin, Q., Xia, H., Xu, Z., Yang, S., 2011. Production of 2,3-butanediol from glucose by GRAS microorganism *Bacillus amyloliquefaciens*. J. Basic Microbiol. 51, 650–658. https://doi.org/10.1002/jobm.201100033.

Yang, T., Rao, Z., Zhang, X., Xu, M., Xu, Z., Yang, S.-T., 2013. Improved production of 2,3-butanediol in *Bacillus amyloliquefaciens* by over-expression of glyceraldehyde-3-phosphate dehydrogenase and 2,3-butanediol dehydrogenase. PloS One 8, e76149. https://doi.org/10.1371/journal.pone.0076149.

Yu, B., Sun, J., Bommareddy, R.R., Song, L., Zeng, A.-P., 2011. Novel (2 *R* ,3 *R*)-2,3-Butanediol dehydrogenase from potential industrial strain *Paenibacillus polymyxa* ATCC 12321. Appl. Environ. Microbiol. 77, 4230–4233. https://doi.org/10.1128/AEM.02998-10.

Yu, E.K.C., Saddler, J.N., 1985. Biomass conversion to butanediol by simultaneous saccharification and fermentation. Trends Biotechnol. 3, 100–104. https://doi.org/10.1016/0167-7799(85)90093-9.

Zeng, A.-P., Byun, T.-G., Posten, C., Deckwer, W.-D., 1994. Use of respiratory quotient as a control parameter for optimum oxygen supply and scale-up of 2,3-butanediol production under microaerobic conditions. Biotechnol. Bioeng. 44, 1107–1114. https://doi.org/10.1002/bit.260440912.

Zhang, L., Cao, C., Jiang, R., Xu, H., Xue, F., Huang, W., Ni, H., Gao, J., 2018. Production of R,R-2,3-butanediol of ultra-high optical purity from *Paenibacillus polymyxa* ZJ-9 using homologous recombination. Bioresour. Technol. 261, 272–278. https://doi.org/10.1016/j.biortech.2018.04.036.

Zhang, L., Yang, Y., Sun, J., Shen, Y., Wei, D., Zhu, J., Chu, J., 2010. Microbial production of 2,3-butanediol by a mutagenized strain of *Serratia marcescens* H30. Bioresour. Technol. 101 https://doi.org/10.1016/j.biortech.2009.10.052, 1961–1967.